Journal Club
June 10, 2015

Recent ALMA results on dust in high-z less massive galaxies

Berger, E., et al. 2014, ApJ, 796, 96
Watson, D. et al. 2015, Nature, 519, 327
Mancini, M. et al. 2015, MNRAS, in press

Kotaro Kohno

IoA/UTokyo

ALMA observations of the host galaxy of GRB 090423 at z=8.23: deep limits on obscured star formation 630 million years after the big bang

Berger, E., et al. 2014, ApJ, 796, 96

We present rest-frame far-infrared (FIR) and optical observations of the host galaxy of GRB 090423 at $z = 8.23$ from the Atacama Large Millimeter Array (ALMA) and the *Spitzer Space Telescope*, respectively. The host remains undetected to 3σ limits of $F_\nu(222\,\mathrm{GHz}) \lesssim 33\,\mu\mathrm{Jy}$ and $F_\nu(3.6\,\mu\mathrm{m}) \lesssim 81\,\mathrm{nJy}$. The FIR limit is about 20 times fainter than the luminosity of the local ULIRG Arp 220 and comparable to the local starburst M 82. Comparing this with model spectral energy distributions, we place a limit on the infrared (IR) luminosity of $L_{\mathrm{IR}}(8\text{–}1000\,\mu\mathrm{m}) \lesssim 3\times10^{10}\,L_\odot$, corresponding to a limit on the obscured star formation rate of $\mathrm{SFR_{IR}} \lesssim 5\,M_\odot\,\mathrm{yr}^{-1}$. For comparison, the limit on the unobscured star formation rate from *Hubble Space Telescope* rest-frame ultraviolet (UV) observations is $\mathrm{SFR_{UV}} \lesssim 1\,M_\odot\,\mathrm{yr}^{-1}$. We also place a limit on the host galaxy stellar mass of $M_* \lesssim 5\times10^7\,M_\odot$ (for a stellar population age of 100 Myr and constant star formation rate). Finally, we compare our millimeter observations to those of field galaxies at $z \gtrsim 4$ (Lyman break galaxies, Lyα emitters, and submillimeter galaxies) and find that our limit on the FIR luminosity is the most constraining to date, although the field galaxies have much larger rest-frame UV/optical luminosities than the host of GRB 090423 by virtue of their selection techniques. We conclude that GRB host galaxies at $z \gtrsim 4$, especially those with measured interstellar medium metallicities from afterglow spectroscopy, are an attractive sample for future ALMA studies of high redshift obscured star formation.

Key words: galaxies: high-redshift – gamma-ray burst: individual (GRB 090423) – radio continuum: galaxies

Constraining FIR/dust properties of the GRB 090423 @z=8.23

- 222 GHz (1.4mm) with ALMA ➔ rest-frame ~150μm (i.e, peak of SED)

25-28 antennas, 160 min on-source

1σ=11μJy

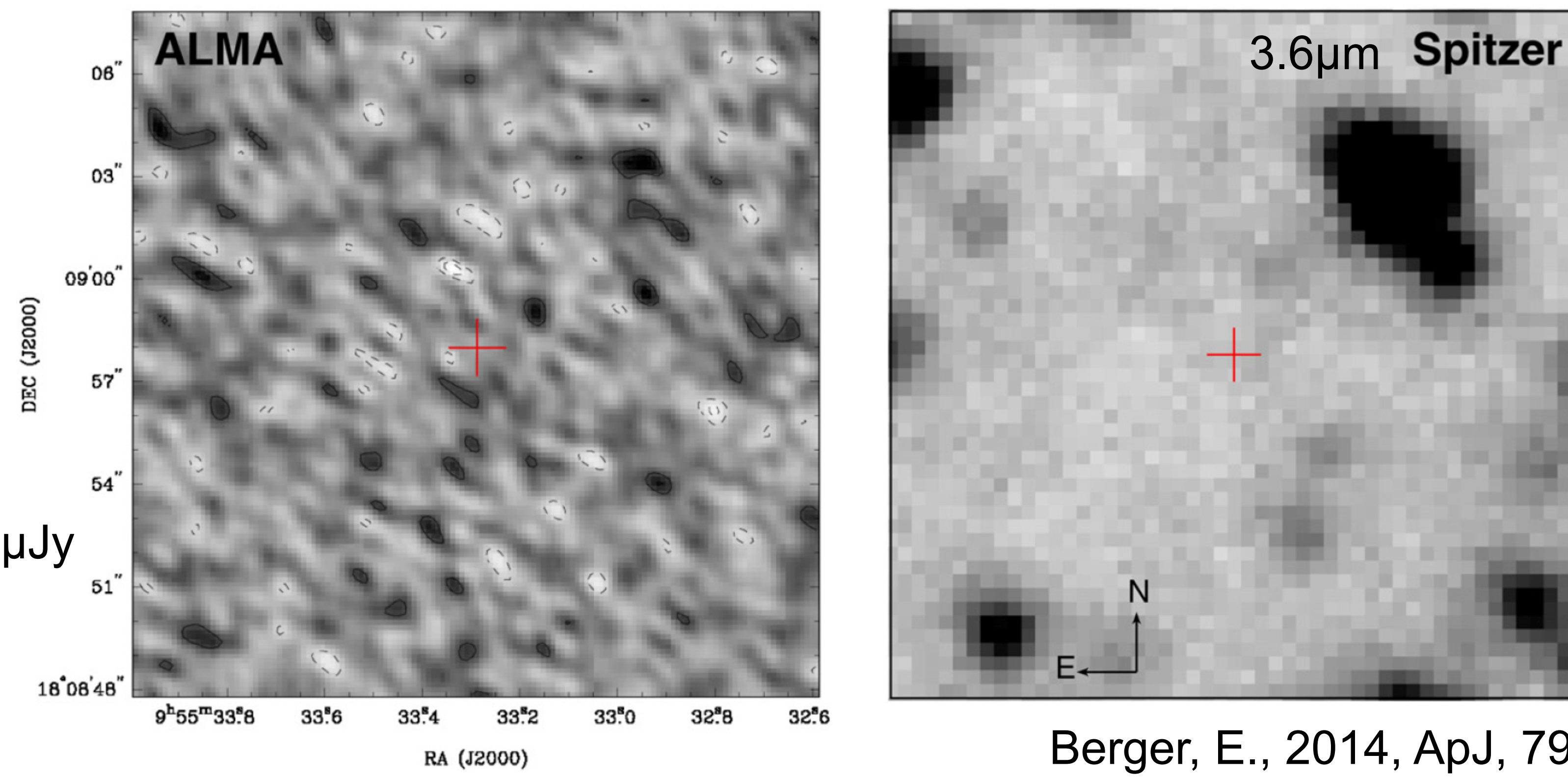

Berger, E., 2014, ApJ, 796 96

Figure 1. Left: ALMA band 6 continuum image of a 20″ × 20″ region centered on the location of the host galaxy of GRB 090423 (cross). Contours are in steps of $1\sigma = 11\ \mu\text{Jy beam}^{-1}$ starting at $\pm 2\sigma$ (solid: positive; dashed: negative). No millimeter emission is detected at the location of the host galaxy. Right: *Spitzer*/IRAC 3.6 μm image of a 20″ × 20″ region centered on the location of the host galaxy of GRB 090423 (cross). No infrared emission is detected at the location of the host galaxy.

Constraints on SED and host properties

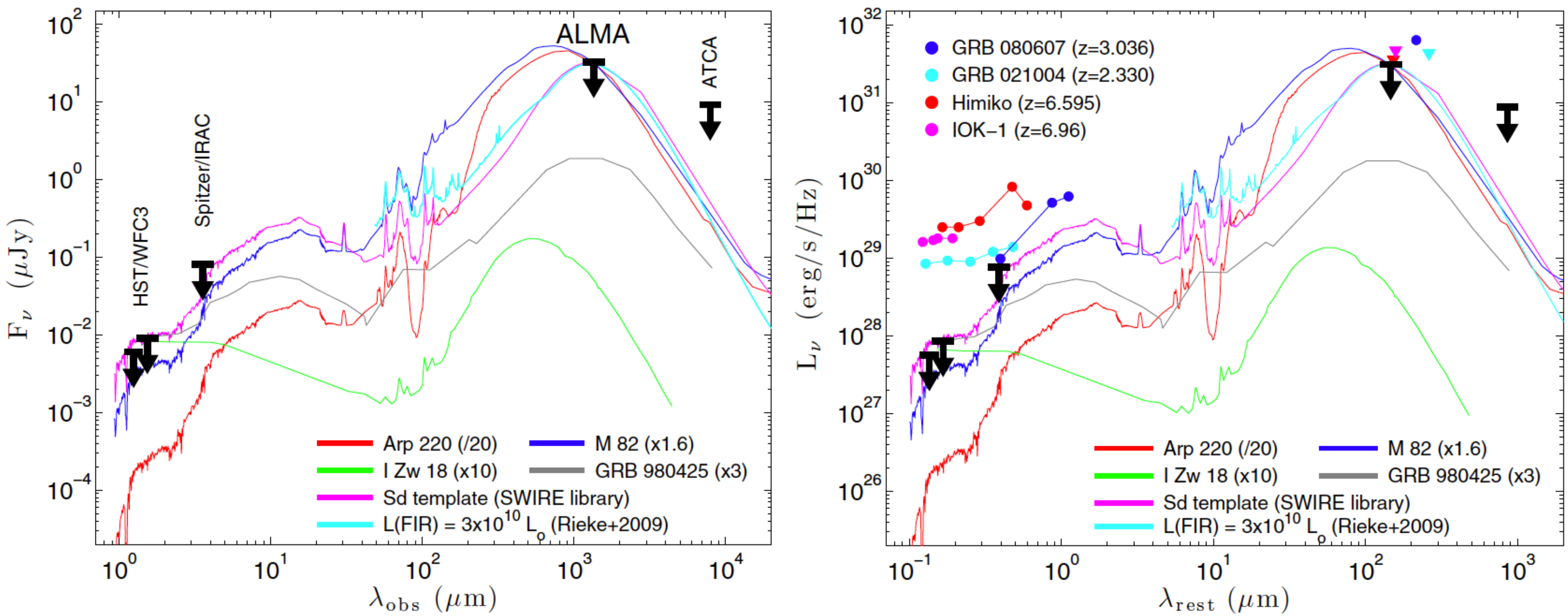

Figure 2. Left: limits on the flux density of the host galaxy of GRB 090423 in the near-IR (*HST*), mid-IR (*Spitzer*), millimeter (ALMA), and radio (ATCA). Also shown are the SEDs of the local ULIRG Arp 220 (red), the local starburst M 82 (blue), the local dwarf I Zw 18 (green), the local host galaxy of GRB 980425 (gray; Michałowski et al. 2014), an Sd galaxy template (magenta), and a template for a galaxy with $L_{IR} = 3 \times 10^{10}\ L_\odot$ (cyan; Rieke et al. 2009), all shifted to $z = 8.23$ with the exception of I Zw 18 and the host of GRB 980425, which are scaled to the *HST* limits. The galaxy models are scaled to match the ALMA flux density limit. For the Arp 220 template, the ALMA non-detection places a stronger constraint on the SED than the *HST* and *Spitzer* limits, while for the starburst templates, the limits are comparable. For the I Zw 18 and GRB 980425 host galaxy templates, the *HST* limits are more constraining. Right: same as the left panel, but plotting the rest-frame luminosity density and wavelength. Also shown are the ALMA observations and rest-frame UV/optical SEDs of two other GRB host galaxies (circles: detections; triangles: upper limits; GRB 080607 is a marginal 3.4σ detection; Wang et al. 2012), and two spectroscopically confirmed LAEs at $z \approx 6.6$–7.0 (Ouchi et al. 2013; Ota et al. 2014).

Berger, E., 2014, ApJ, 796 96

Constraints on SED and host properties

- Modified blackbody SED
  - Tdust = 30 – 50 K, β = 1.5 – 2
  - Lower boundary of Tdust: $T_{CMB}(z=8.23) = 25K$

Parameter	Value
L_{IR}^{a}	$\lesssim(2–5) \times 10^{10}\ L_{\odot}$
SFR_{IR}^{a}	$\lesssim 3–5\ M_{\odot}\ yr^{-1}$
SFR_{UV}^{rmb}	$\lesssim 1.2\ M_{\odot}\ yr^{-1}$
M_{*}^{c}	$\lesssim(1–5) \times 10^{7}\ M_{\odot}$

Notes.
[a] Assuming $T_{dust} \approx 30–50$ K and $\beta \approx 1.5–2$.
[b] Assuming $A_V^{host} = 0$ mag.
[c] Assuming a stellar population age of 10–100 Myr, constant star formation rate, Salpeter IMF, $Z = 0.2\ Z_{\odot}$, and $A_V^{host} = 0$ mag.

Berger, E., 2014, ApJ, 796 96

Comparison with other high-z galaxy populations

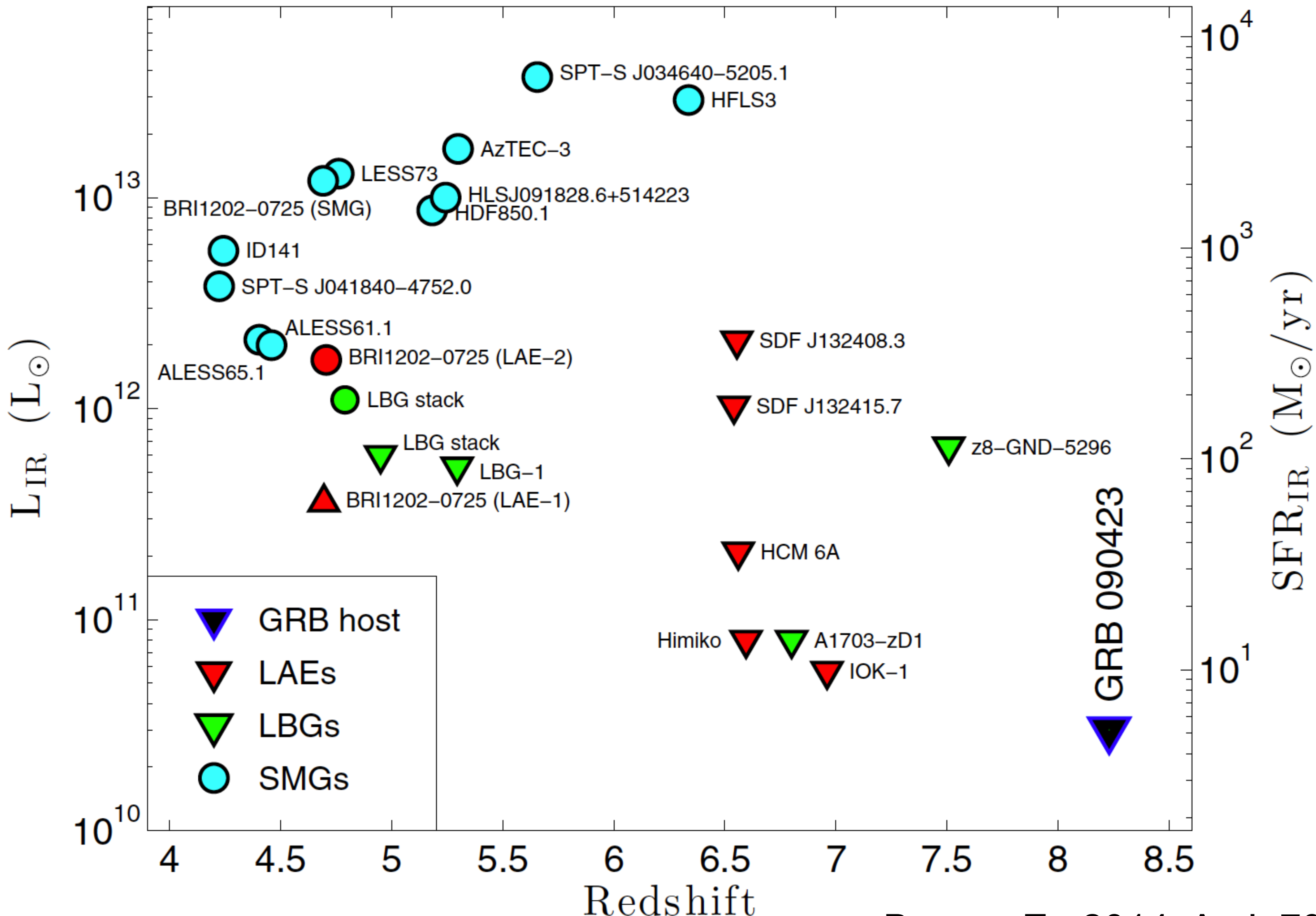

Berger, E., 2014, ApJ, 796 96

A dusty, normal galaxy in the epoch of reionization

Candidates for the modest galaxies that formed most of the stars in the early Universe, at redshifts $z > 7$, have been found in large numbers with extremely deep restframe-ultraviolet imaging[1]. But it has proved difficult for existing spectrographs to characterize them using their ultraviolet light[2–4]. The detailed properties of these galaxies could be measured from dust and cool gas emission at far-infrared wavelengths if the galaxies have become sufficiently enriched in dust and metals. So far, however, the most distant galaxy discovered via its ultraviolet emission and subsequently detected in dust emission is only at $z = 3.2$ (ref. 5), and recent results have cast doubt on whether dust and molecules can be found in typical galaxies at $z \geq 7$[6–8]. Here we report thermal dust emission from an archetypal early Universe star-forming galaxy, A1689-zD1. We detect its stellar continuum in spectroscopy and determine its redshift to be $z = 7.5 \pm 0.2$ from a spectroscopic detection of the Lyman-α break. A1689-zD1 is representative of the star-forming population during the epoch of reionization[9], with a total star-formation rate of about 12 solar masses per year. The galaxy is highly evolved: it has a large stellar mass and is heavily enriched in dust, with a dust-to-gas ratio close to that of the Milky Way. Dusty, evolved galaxies are thus present among the fainter star-forming population at $z > 7$.

Watson, D. et al. 2015, Nature 519, 327

VLT spectroscopy

- Target: A1689-zD1, behind the lensing galaxy cluster Abell 1689
  - A candidate z>7 system from deep imaging with HST and Spitzer; z-photo = 7.6 ± 0.4
  - Gravitationally magnified by a factor of 9.3
  - One of the brightest candidate z > 7 candidate known
- X-shooter spectroscopy
  - March 2010 and March 2012, 16 hours on target

NIR spectrum of A1689-zD1

- One of the most distant galaxies known to be confirmed via spectroscopy
- The only galaxy at z>7 where the redshift is determined from spectroscopy of its stellar continuum

No line
Rest-frame EW < 4Å for Lyα & CIII]

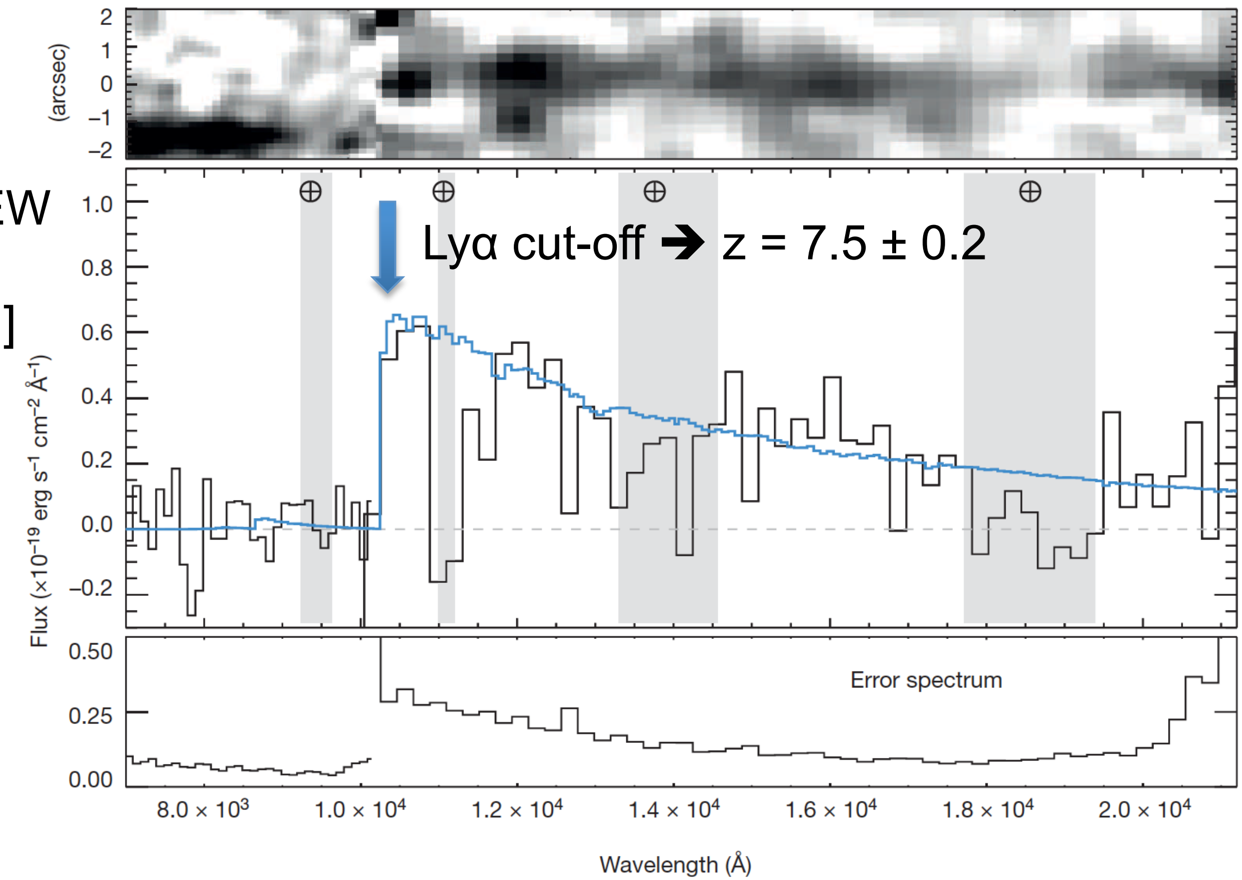

"blue" spectrum
$F_\lambda \propto \lambda^{-\beta}$
B = 2.0 ± 0.1

Figure 2 | Spectrum of A1689-zD1. The binned one-dimensional (middle panel) and two-dimensional (upper panel; wavelength versus distance along the slit) spectra are shown, with the 68% confidence uncertainty for the one-dimensional spectrum in the bottom panel. The redshift $z = 7.5$ is determined from the Lyα break at 1,035 nm. Sky absorption (grey bands) and the best-fit SED (blue line) are shown. The Lyα break is close to the spectrograph's near-infrared (NIR)/visual (VIS) arm split; however, the break is clearly detected in the NIR arm alone. A nearby galaxy ($z \approx 2$) visible in the bottom part of the two-dimensional spectrum is detected in both the VIS and the NIR arms.

ALMA detection of a dusty source at z=7.5±0.2 behind the cluster Abell 1689

ALMA 1.3mm
0.61±0.12 mJy

cy0 + cy1

Watson et al. 2015, Nature 519, 327

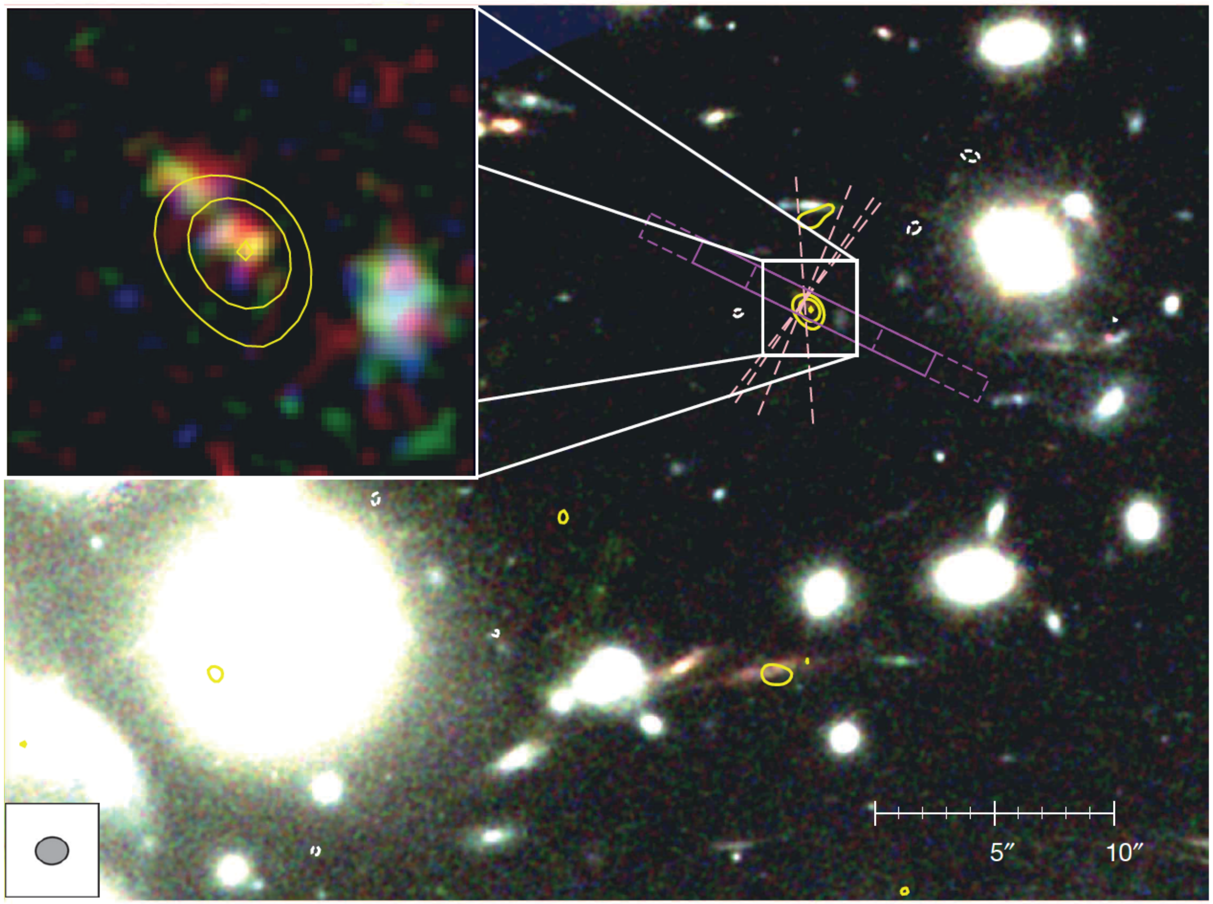

Figure 1 | The gravitationally lensing galaxy cluster Abell 1689. The colour image is composed with Hubble Space Telescope filters: F105W (blue), F125W (green) and F160W (red). The zoomed box ($4'' \times 4''$) shows A1689-zD1. Contours indicate far-infrared dust emission detected by ALMA at 3σ, 4σ, and 5σ local rms (yellow, positive; white, negative). The ALMA beam ($1.36'' \times 1.15''$) is shown, bottom left. Images and noise maps were primary-beam corrected before making the signal-to-noise ratio (SNR) maps. Slit positions for the first set of X-shooter spectroscopy are overlaid in magenta (dashed boxes indicate the dither), while the parallactic angle was used in the remaining observations (pink dashed lines).

ALMA observations

- 211 GHz + 241 GHz
- The source is located towards the northern edge of the mosaic (42% of the sensitivity of the deepest part of the mosaic)
- The source is brightest in the mosaic area of 5 arcmin^2

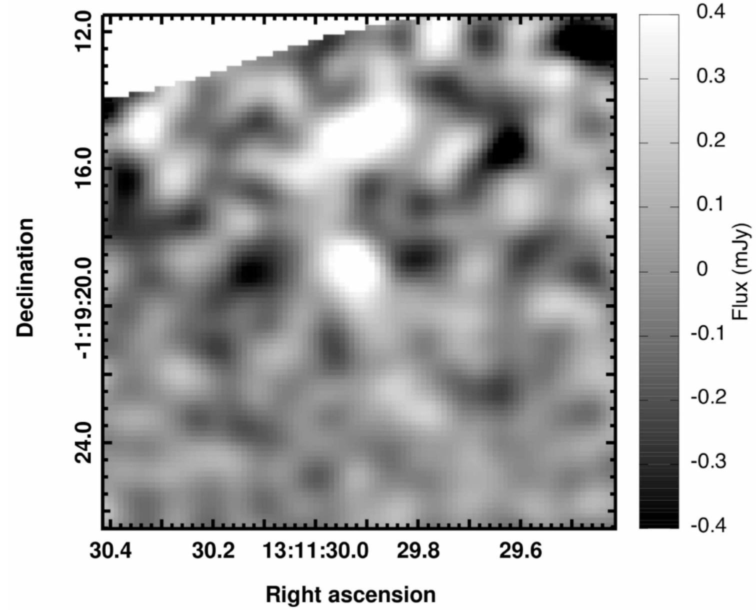

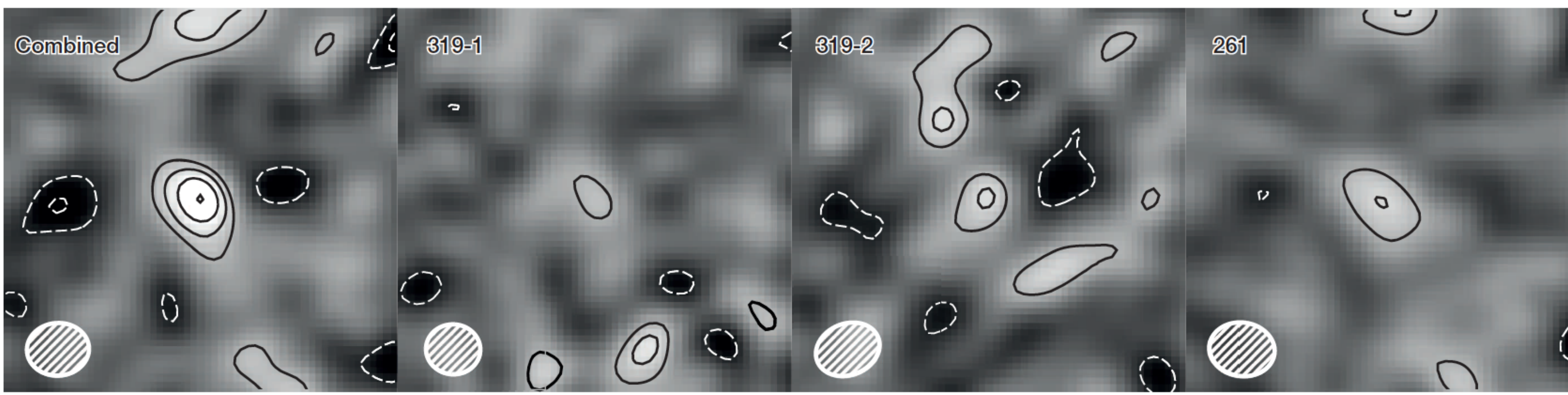

Figure 3 | ALMA SNR maps of A1689-zD1. Contours are SNR = 5, 4, 3, 2 (black, solid), −3, −2 (white, dashed). Images and noise maps were primary-beam corrected before making SNR maps. Beam sizes are shown at the bottom left of each panel. Panels are 8″ × 8″. The panels show from left to right: the combined data, the two tunings of observation 2011.0.00319.S and observation 2012.1.00261.S. A1689-zD1 is detected from left to right, at 5.0σ, 2.4σ, 3.1σ, and 3.0σ. Natural weighting was used and the visibilities were tapered with a 1″ circular Gaussian kernel, resulting in beams of 1.36″ × 1.15″, 1.19″ × 1.09″, 1.43″ × 1.12″, 1.43″ × 1.17″ from left to right.

L(UV) = $1.8\times10^{10}L_{\odot}$
➔ SFR(UV) =
$2.7 \pm 0.3\ M_{\odot}$/yr
fainter than L* !

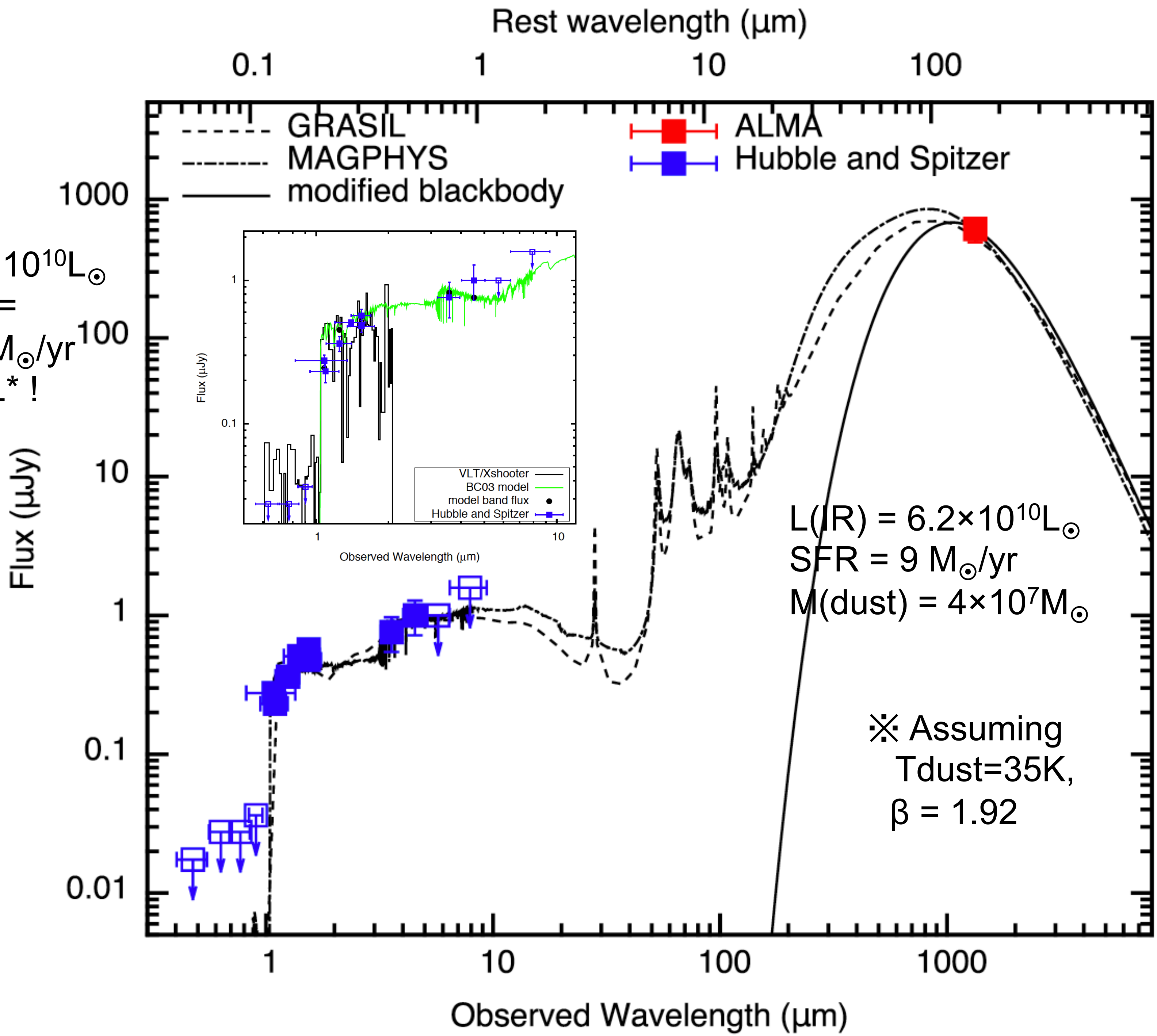

Comparison with other high-z star-forming galaxies

Mancini et al. 2015, MNRAS, in press
arXiv: 1505.01841

Name	z	M_{UV} mag	Log M_{star} [$M_\odot$]	Log M_{dust} [$M_\odot$]
A1703-zD1[a]	6.800	-20.3	9.2 ± 0.3	< 7.36
z8-GND-5296[a]	7.508	-21.4	9.7 ± 0.3	< 8.28
HCM6A[b]	6.560	-20.8	9.5 ± 0.3	< 7.61
IOK-1[c]	6.960	-21.3	9.7 ± 0.3	< 7.43
Himiko[d]	6.595	-21.7	9.9 ± 0.3	< 7.30
BDF-3299[e]	7.109	-20.44	9.3 ± 0.3	< 7.02
BDF-512[e]	7.008	-20.49	9.3 ± 0.3	< 7.36
SDF-46975[e]	6.844	-21.49	9.8 ± 0.3	< 7.38
A1689-zD1[f]	7.500	-19.7	9.0 ± 0.3	7.51 ± 0.2

Table 1 | Comparison of A1689-zD1 to other high-*z* star-forming galaxies

Galaxy name	Redshift, z	Stellar mass, $M_\star$ ($10^9 M_\odot$)	SFR_{UV} ($M_\odot$ yr^{-1})	$SFR_{Ly\alpha}$ ($M_\odot$ yr^{-1})	SFR_{IR} ($M_\odot$ yr^{-1})	Dust mass, M_D ($10^7 M_\odot$)
HFLS3 (ref. 21)	6.34	50^{+100}_{-30}	1.3 ± 0.4*	—	$1,300_{-520}$†	30_{-10}†
HCM6A (ref. 22)	6.56	—	9 ± 2	2	<28 (ref. 26)	<10 (ref. 26)
Himiko (ref. 8)	6.60	15 ± 2	30 ± 2	35 ± 1	<8	<4.72 (ref. 26)
A1703-zD1 (ref. 23)	6.8	0.7–1.5	7.3 ± 0.3	—	<16 (ref. 26)	<5.7 (ref. 26)
IOK-1 (ref. 24)	6.96	<40	23.9 ± 1.4 (ref. 27)	10 ± 2	<10 (ref. 28)	<6.4 (ref. 28)
z8-GND-5296 (ref. 2)	7.51	$1^{+0.2}_{-0.1}$	330^{+710}_{-10}	—	<127 (ref. 26)	<50 (ref. 26)
HG090423 (ref. 25)	8.2	<0.05 (ref. 29)	<0.38 (ref. 30)	—	<5 (ref. 29)	<2‡
A1689-zD1	**7.5**	$\mathbf{1.7^{+0.7}_{-0.5}}$	$\mathbf{2.7 \pm 0.3}$	**<0.7**	$\mathbf{9^{+4}_{-2}}$	$\mathbf{4^{+4}_{-2}}$

The SFRs are derived from extinction-uncorrected ultraviolet emission, Lyα emission and far-infrared emission, respectively.
* Derived from the Hubble Space Telescope F160W photometry and corrected for lensing.
† 95% lower bound only.
‡ Assuming the same dust parameters assumed for A1689-zD1.

Watson et al. 2015, Nature, 519, 327

Physical properties of A1689-zD1

- FIR detection at $z=7.5$ ➔ must have enriched its interstellar media with metals and dust
- Metals: primarily produced and distributed via supernova explosions ➔ metal enrichment happens concurrently with massive star formation
- The site of dust production: less certain

The mechanism must be very rapid!

The strongest direct constraints on the rapidity of dust enrichment, occurring within only 500 million years of the beginning of star formation in the Universe.

The dust mass in z > 6 normal star forming galaxies

Mancini, M., et al. 2015, MNRAS, in press (arXiv: 1505.01841)

ABSTRACT

We interpret recent ALMA observations of $z > 6$ normal star forming galaxies by means of a semi-numerical method, which couples the output of a cosmological hydrodynamical simulation with a chemical evolution model which accounts for the contribution to dust enrichment from supernovae, asymptotic giant branch stars and grain growth in the interstellar medium. We find that while stellar sources dominate the dust mass of small galaxies, the higher level of metal enrichment experienced by galaxies with $M_{star} > 10^9\,M_\odot$ allows efficient grain growth, which provides the dominant contribution to the dust mass. Even assuming maximally efficient supernova dust production, the observed dust mass of the $z = 7.5$ galaxy A1689-zD1 requires very efficient grain growth. This, in turn, implies that in this galaxy the average density of the cold and dense gas, where grain growth occurs, is comparable to that inferred from observations of QSO host galaxies at similar redshifts. Although plausible, the upper limits on the dust continuum emission of galaxies at $6.5 < z < 7.5$ show that these conditions must not apply to the bulk of the high redshift galaxy population.

Key words: dust, extinction galaxies: evolution galaxies: high-redshift galaxies: ISM ISM: supernova remnants submillimetre: galaxies

Very efficient grain growth is required!

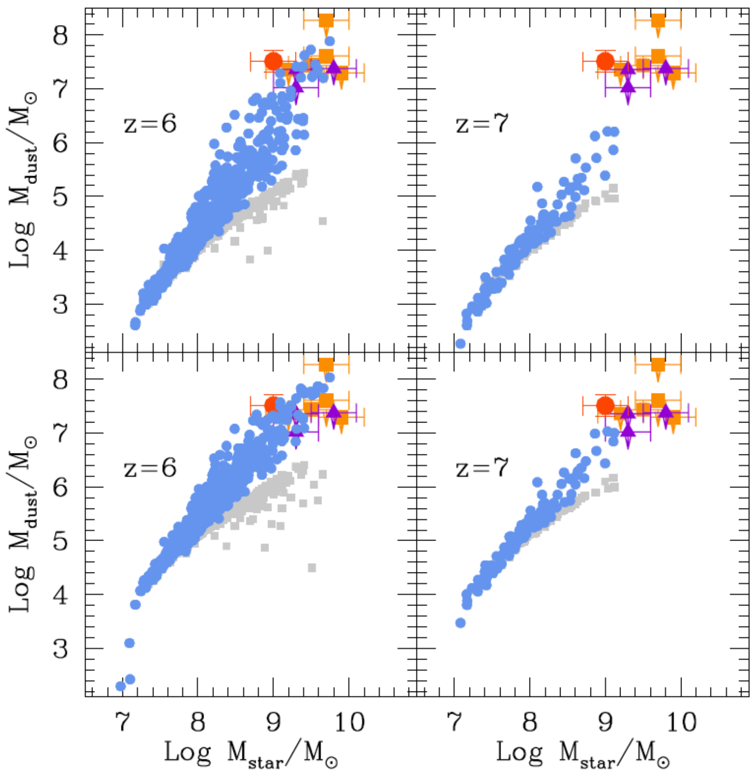

Figure 1. Predicted dust masses of the simulated galaxies as a function of the stellar mass. For each galaxy, the dust mass without (with) grain growth is shown by a square grey (circle blue) point (see text). The adopted grain growth timescale is $\tau_{acc,0} = 2\,\mathrm{Myr}$. In the lower panels, the reverse shock destruction of SN dust is neglected. For the sake of comparison, we have reported the same data points shown in Table 1 in the two panels: Schaerer et al. (2015, squares), Maiolino et al. (2015, triangles) and Watson et al. (2015, circle point).

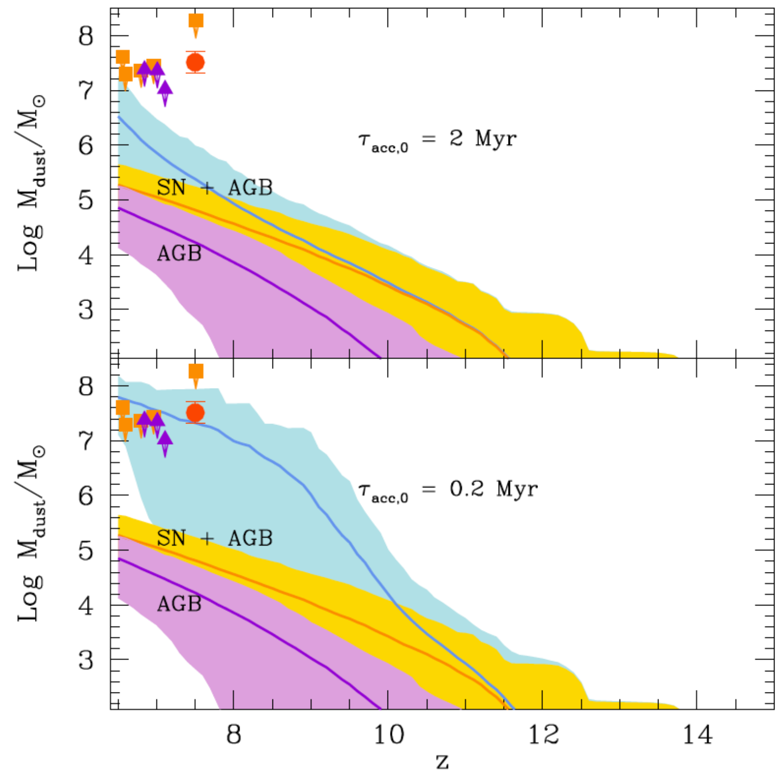

Figure 2. Redshift evolution of the dust mass for the simulated galaxies with stellar masses in the range Log $M_{star}/M_{\odot} \geq 9$. Each line represents the average contribution of all the galaxies with the shaded area indicating the dispersion among different evolutionary histories. The lower, intermediate and upper lines show the contribution to the total mass of dust of AGB stars, stellar sources and grain growth with an accretion timescale of $\tau_{acc,0} = 2\,\mathrm{Myr}$ (upper panel) and 0.2 Myr (lower panel).

Mancini et al. 2015, MNRAS, in press
arXiv: 1505.01841